TIM: Tree Imaging Machine

Your Name

February 9, 2025

Abstract

The Tree Imaging Machine (TIM) is a do-it-yourself scanning tool made to digitize tree cookies and cores. TIM takes partially overlapping microscopic images of samples and stitches the individual images together to form a mosaic. These mosaics can be zoomed in to see distinct features on the scale of 0.01mm. With scans of up to 21,140 DPI, TIM produces one of the highest resolution images among similar tools for the competitive price of less than $3,000 USD. We designed TIM to have a large working plane to allow the digitization of individual cores over 50cm and to allow the operator to set a batch of samples to be digitized without intervention. All of the 3D printed parts are available for download on the NIH 3D printing repository and the software is open source. Instructions to recreate this tool can be found on the code repository.

1 Introduction

The study of tree rings is useful across multiple fields, proving to be a reliable method for reconstructing past climates of regional and local environments, as well as a mechanism to understand tree growth response [1] [16] [5] [15]. To obtain these data from the tree rings, it is necessary to measure tree rings widths from a tree cookie or core. The first high precision tool for this purpose was a stage micrometer, involving a trained technician to incrementally shift a tree core under the objective of a microscope - informing a computer when a new ring is encountered [14]. While this method has very high precision, the data is only as accurate as the experience and knowledge of the technician at the time of recording [6]. The desire to remove repetition of errors in sampling and sampling bias across to individual technicians led researchers to an alternative - image analysis.

The first step in measuring tree ring width from images requires the digitization of the sample from one of two major methods. The original technique was as a flatbed scanner which can digitize the entire sample at once [4]. With a top of the line scanner, like the Epson Perfection V850 Pro, it's possible to scan at maximum resolutions of 4800 dpi and scan an area of up to 8.5" x 11.7" (21.6cm x 29.7cm). Analysis which relies on higher resolution or of larger samples require a different digitization approach.

The second digitization model was introduced with ATRICS [6]. Rather than scanning a whole sample at once, a high resolution camera takes multiple images across the surface of the sample and uses image stitching software techniques to combine them into one ultra high resolution image [10]. Stitching multiple images into one mosaic has been applied in other fields such as mineralogy and cellular biology [13, 9]. This method requires either the camera objective to move relative to the sample, or the sample move

underneath a stationary camera. For ATRICS and a more modern do-it-yourself alternative, CaptuRING, the sample is moved relative to the camera [2]. Gigapixel takes a different approach by moving the camera relative to the sample, allowing for multiple samples to be recorded in sequence [3]. While these machines can all digitize cores, none have been shown to digitize cookies.

TIM was made to combine the defining features of the previously mentioned machines into one while making the project open-source and open-hardware. We designed TIM to digitize both cookies and cores, increase the maximum sample length, perform image stitching without operator intervention, and capture batches of samples in a queue - all while minimizing cost. The only specialized piece of equipment needed to build TIM is a 3D printer, but the parts can be readily ordered through 3D print shops if preferred. Excluding 3D printed parts, the total cost of the machine is approximately $2,200 USD compared to the $70,000 USD of the Gigapixel [3]. The total cost of the machine is almost comparable in price or less to many professional camera and macro lens combinations. Additional savings can also be had when factoring in the cost of a professional stitching software license such as PTGui.

2 Methods

2.1 System Overview

TIM can be thought of as a combination of multiple subsystems: the camera, computer, and gantry machine. Cartesian movement in the X, Y and Z directions is a result of two machine kits and a motor controller from OpenBuilds - the ACRO 1010, the NEMA 17 lead screw linear actuator, and the X32 Motor Controller running GRBL firmware. Smaller and larger working planes easily be achieved by purchasing a different sized ACRO kit. Building on top of kits allowed for quick assembly with sound instructions and saved development time. To fit on the build plates of the ACRO system, we made an adapter to connect the linear actuator to the X and Y axis, thus creating motion in the Z axis. On the linear actuator's build plate, adapters were made to hold a 12MP Raspberry Pi HQ Camera equipped with a SEEED studio microscope lens connected to an NVIDIA Jetson Orin Nano (Jetson) through a CSI cable. By choosing this combination, we were able to reduce the weight and cost of the camera significantly - trickling the budget into an efficient computer which can handle intensive image processing. The Jetson is a powerful edge computer which drives a monitor for a GUI, sends commands to the motor controller to move the machine, runs image processing calculations for automatic control, and performs calculations to stitch individual images into one mosaic. Despite the weight reductions, torsion on the gantry arm still resulted in a non-zero torsional deflection. A torsion correcting adapter was designed to counteract this rotation and level the lens.

2.2 Preparing Cookies and Cores

TIM can be used to scan both tree cookies and tree cores. Sample preparation for both are equally important but require different approaches. The scanning surface of the cookies and cores need to be sanded with incrementally increasing sand paper grit. Our cookies were sanded using an orbital sander with mesh sandpaper from 60 to 800 grit. We used a microscope to visually inspect the quality of the sanding and when vessels were easily identifiable, we considered the sample to be sufficiently prepared.

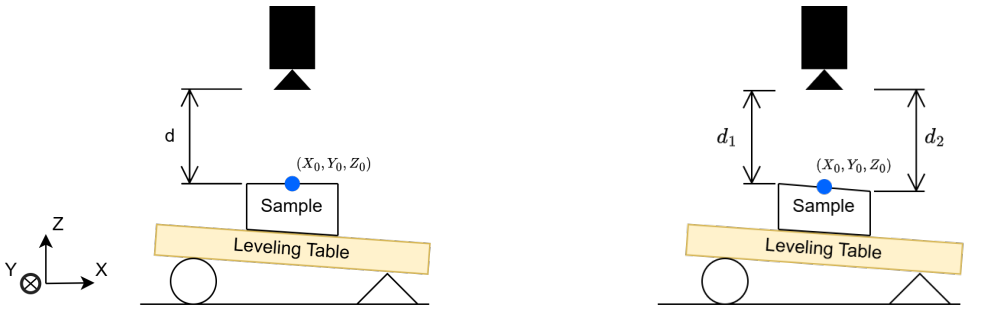

(a) Ideal sample leveling

(b) Realistic sample leveling

Figure 1: Side view of the camera and sample on top of a leveling table. The ideal sample leveling shows a uniform distance d at all (X, Y) coordinates on the sample. This is impossible to achieve in reality, the true sample leveling has a non uniform distance at unique (X_i, Y_i).

Special sanding considerations need to be taken for each sample type. For cookies, it is important to have the top and bottom surfaces be nearly parallel. Small differences in plane angle can be corrected using the 3D printed levelling table we designed (See Figure 1a). For cores, care should be taken to maximize the scanning surface. This means removing material to be coincident to the center of the cross section of the core. Similarly to cookies, care should be given to achieving a scanning surface as parallel to the XY-plane as possible. Cores also need to be aligned to be parallel to the Y axis to be digitized, using squaring tool or similar to help with alignment. Any warping in core mounts need to be counteracted with the use of trigger clamps.

2.3 Sample Digitization

The subsystems can be best understood by following the process from sample setup through through obtaining a stitched image. To achieve this with a fixed focus camera, the samples must be nearly orthogonal to the camera lens. Once the sample is level, the operator interacts with the machine through the GUI to navigate the camera to the center of the sample, and focuses the preview image to be sharp by moving in the Z axis. The height and width dimensions are then entered in the GUI to be saved along with the detected center coordinate of the sample. This procedure can be repeated to create a queue of samples to digitize as a batch. The height, width, identifiers, sample type, and centering of the sample is sufficient information to digitize.

2.4 Image Capturing

In the GUI the operator indicates the height and width of the field of view in an individual image from the camera. This varies on the focal length of the lens, but we have kept the field of view to be 3mm x 5mm. Once prompted the system begins to exhaustively traverse the surface area of the sample, using the sample height and width entered by the operator. The goal of this traversal is to obtain in-focus images that have a region of overlap with all its neighbors - the basis of image stitching. Digitizing cores can be done without needing to traverse in both the X and Y axis. The optimal scanning path for a core is to ignore the Y axis and traverse the cores length. Spanning the surface area of a cookie requires movement in both the X and Y axis.

By centering the design around a fixed focus camera and lens, it is necessary to implement automatic control to focus the images. The only way to control the focus of a fixed focus lens is by changing the lens's distance to the sample. And with the microscope lens, the depth of field of the image is so sensitive that sub millimeter heights can move an entire image out of focus. Solving this in a time efficient manner involves two stages. The first stage takes advantage of the requirement to navigate and focus the camera to the center of the sample. This allows the initial Z_0 value ,captured when adding a sample, to be an informed guess as to what value would have an in focus image across the entire surface. From the first (X_0, Y_0) coordinate captured, 11 images are taken at different Z values in $\boldsymbol{Z}_{\text{samples}}$. So long as $Z_{focused}$ is within this set, an in focus image exists.

$$Z_{focused} \in \boldsymbol{Z}_{\text{samples}} = Z_0 + \begin{bmatrix} -0.5 \\ -0.4 \\ \vdots \\ 0.4 \\ 0.5 \end{bmatrix}$$

Our focusing procedure begins at 0.5 mm above Z_0 and finishes with the last image at 0.5 mm below Z_0. The 11 images then have their normalized variance, NV, calculated in a separate thread to measure the image sharpness [8]. The image with the maximum score is saved and can be considered the most in focus image, while the rest are deleted from storage.

$$i_{\max} = \arg\max_i NV(image(\boldsymbol{Z}_{\text{focus}}))$$

This focusing procedure works well alone when the sample alignment has a difference in height no greater than 0.5 mm, $d_1 - d_2 < 0.5mm$ (See Figure 1b). Rather than adjusting this range, a greater alignment error can be managed by controlling the center of the range, $Z_{0,k}$, for (X_k, Y_k). The likelihood of an adjacent (X_{k+1}, Y_{k+1}) containing an in focus image is highest when the current $i_{\max,k}$ is at the middle index of $\boldsymbol{Z_{samples}}$. A PID control algorithm with a process variable of i_{max} and control variable of $Z_{0,k}$ allows a negative feedback loop to improve focusing across the entire sample [11]. Instead of $(Z_{max} - Z_{min}) < 0.5mm$, now the system can handle $(Z_k - Z_{k+1} < 0.5mm)$ which allows for a more forgiving sample setup. After the capturing overlapping images across the entire surface area, the images are ready to be stitched.

To reduce motion blur in the images, the range of $\boldsymbol{Z}_{\text{samples}}$ is traversed at constant velocity and images are captured without stopping. Decoupling the auxiliary camera control from the G-code commands to control the machine has shown to improve speed and decrease vibrational effects from acceleration and deceleration [12]. This is a variation of the standard approach used in 3D printing and CNC control methods.

2.5 Accounting for Translation Error Between Core Samples

Difficulties arise when more than one core are added to the digitization queue. The ACRO has a theoretical 4.5 micron translational accuracy, but is hard to achieve. These inaccuracies can cause drift in the images with relation to the core and result in the width of the core not being within the field of view of the images. Specifically for cores, a centering procedure was implemented to realign the center of the core to the center of the image frame when the machine moves to a new sample.

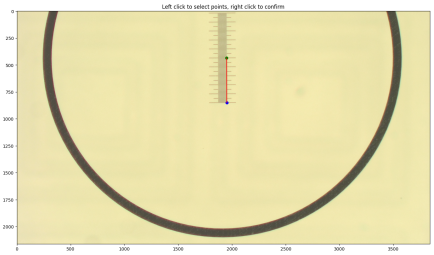

(a) Scale Bar for DPI measurements

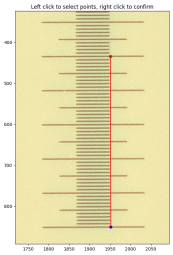

(b) Zoomed in Scale Bar

Figure 2: Example of a single DPI measurement using a 0.01mm slide scale. The DPI was measured at multiple locations in the field of view both vertically and horizontally. They converged on the same value.

First, the camera is moved to to the (X_0, Y_0, Z_0) of the new core. From there, the camera is moved across a window, at constant velocity, from $(X_0 - 1/2 * range, Y_0, Z_0)$ to $(X_0 + 1/2 * range, Y_0, Z_0)$. Images are captured at equal distance intervals analogously to the image focusing procedure. Once again, the image with the highest normalized variance score is considered the best image and its location is used as the realigned X_0'. This procedure drastically improves digitization quality of batches of cores.

2.6 Stitching

Image stitching is a well explored field, ranging from panoramic images taken on smart phones to highly tuned microscopy slide stitching. But the basis of stitching remains the same across algorithms. Adjacent images must have a region of overlap. Of the stitching tools with a software API that we tested, only the Python package Stitch2D was able to stitch our images successfully into a grid. This package wraps OpenCV functions for finding distinctive image features using the SIFT feature detector and matches these feature within the overlapping region of adjacent images [7]. The default implementation of the package works very well but has an $O(2n)$ space complexity and fails due to out-of-memory errors when stitching hundreds of images. With a few key memory conscious changes to the algorithm, the space complexity was reduced to approximately $O(\log n)$ and the package was able to run on the Jetson without a problem.

Depending on the analysis, it is unnecessary to digitize samples at a very high DPI. To address this, a parameter in the machine configuration file allows the user to downsize images before they get stitched together to avoid unnecessary sample detail and decrease the size of the files. With the same images, multiple final stitched resolutions can be made.

3 Results

TIM is capable of producing extremely high resolution scans. A microscopy slide scale with 0.01mm graduations was used to calculate the dots per inch (DPI) of individual images captured from the system (Figure 2). Using this scale we calculated the maximum DPI to be 21,140. This calculation can be replicated using the Python tool we created as necessary for varied lens focal lengths. When downscaling the final stitch, DPI scales

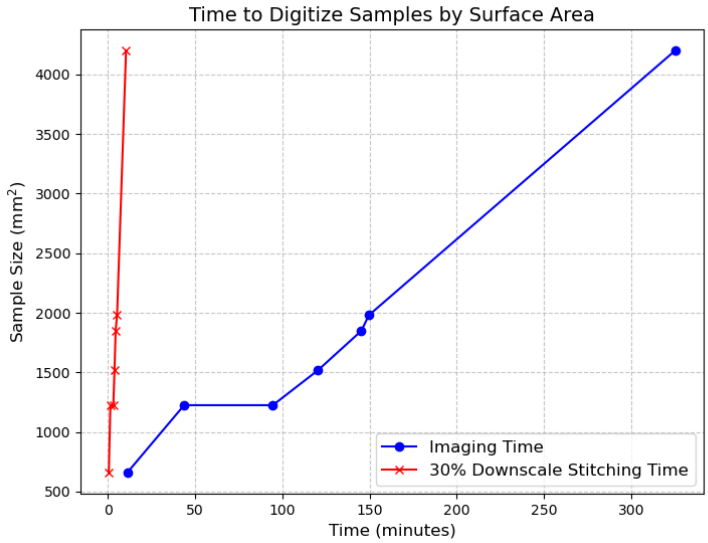

Figure 3: Time to digitize a sample is dependent on the sample's surface area and the desired final resolution. Cores benefit from linear surface area to sample length. The range of sample included are from a 3mm x 220mm core to a 75mm x 56mm cookie. True sampling times are drastically influenced by configurable machine parameters.

linearly with the downscale percentage defined in the machine parameters.

TIM has been used to digitize 90 cookies and is in the process of finishing 1,200 cores. Digitizing samples takes significantly longer for cookies than it does for cores (Figure 3). This is due to the surface area of cookies requiring more images as it has a square relationship to sample radius. For large cookies, the operator can choose to selectively scan a portion of the cookie. Scanning cookies at maximum resolution is unrealistic as the max cookie size is very small. To fit into the maximum 2.5 GB limits of a TIFF file, the maximum diameter of a cookie scanned at 30% of maximum resolution is limited to approximately 130 mm. For cores at maximum resolution, this file size limit constrains samples to approximately 1,500 mm in length. Note that a larger ACRO frame would be needed to support this sample length. Samples that are larger than this file size limit are still possible to be scanned but they are no longer stored as a TIFF file. An uncompressed binary NumPy memory-mapped array file is produced. This implies that the operator knows how to splice into these files and is comfortable working with NumPy memory-mapped arrays in Python.

4 Discussion

By taking advantage of a common 3 degree of freedom cartesian machine design, powerful edge computing, and a microscope camera we were able to design a cost effective and high resolution digitization tool for wood samples. We significantly increased the maximum sample length and maximum resolution compared to common alternatives in the field. In addition, the machine design was intended to be readily replicated by labs with minimal engineering experience and equipment.

4.1 Strengths and Opportunities

Our design has tried to minimize the barriers to building this machine in smaller labs. After investing a few hours in the sourcing and assembly of parts, the rest of the implementation has been completed. Digitized samples from this machine have been able to have tree rings registered onto their images using CooRecorder. Integration into a cloud data storage system would be a great addition to remove the need for an operator to move the final data with a physical external drive. Further testing with vessel counting models or ring identification models would be an interesting extension to take advantage of high resolution scans.

References

[1] Harold C. Fritts. Dendroclimatology and dendroecology. *Quaternary Research*, 1(4): 419–449, December 1971. ISSN 0033-5894. doi: 10.1016/0033-5894(71)90057-3. URL https://www.sciencedirect.com/science/article/pii/0033589471900573.

[2] Miguel García-Hidalgo, Ángel García-Pedrero, Daniel Colón, Gabriel Sangüesa-Barreda, Ana I. García-Cervigón, Juan López-Molina, Héctor Hernández-Alonso, Vicente Rozas, José Miguel Olano, and Víctor Alonso-Gómez. CaptuRING: A do-it-yourself tool for wood sample digitization. *Methods in Ecology and Evolution*, 13(6):1185–1191, 2022. ISSN 2041-210X. doi: 10.1111/2041-210X.13847. URL https://onlinelibrary.wiley.com/doi/abs/10.1111/2041-210X.13847. _eprint: https://onlinelibrary.wiley.com/doi/pdf/10.1111/2041-210X.13847.

[3] Daniel Griffin, Samantha T. Porter, Matthew L. Trumper, Kate E. Carlson, Daniel J. Crawford, Daniel Schwalen, and Colin H. McFadden. Gigapixel Macro Photography of Tree Rings. *Tree-Ring Research*, 77(2):86–94, July 2021. ISSN 1536-1098, 2162-4585. doi: 10.3959/TRR2021-3. URL https://bioone.org/journals/tree-ring-research/volume-77/issue-2/TRR2021-3/Gigapixel-Macro-Photography-of-Tree-Rings/10.3959/TRR2021-3.full. Publisher: Tree-Ring Society.

[4] Régent Guay, Réjean Gagnon, and Hubert Morin. A new automatic and interactive tree ring measurement system based on a line scan camera. *The Forestry Chronicle*, 68(1):138–141, February 1992. ISSN 0015-7546, 1499-9315. doi: 10.5558/tfc68138-1. URL http://pubs.cif-ifc.org/doi/10.5558/tfc68138-1.

[5] Frédéric Guibal and Joël Guiot. Dendrochronology. In Gilles Ramstein, Amaëlle Landais, Nathaelle Bouttes, Pierre Sepulchre, and Aline Govin, editors, *Paleoclimatology*, pages 117–122. Springer International Publishing, Cham, 2021. ISBN 978-3-030-24982-3. doi: 10.1007/978-3-030-24982-3_8. URL https://doi.org/10.1007/978-3-030-24982-3_8.

[6] Tom Levanič. Atrics – A New System for Image Acquisition in Dendrochronology. *Tree-Ring Research*, 63(2):117–122, December 2007. ISSN 1536-1098, 2162-4585. doi: 10.3959/1536-1098-63.2.117. URL https://bioone.org/journals/tree-ring-research/volume-63/issue-2/1536-1098-63.2.117/Atrics--A-New-System-for-Image-Acquisition-in-Dendrochronology/10.3959/1536-1098-63.2.117.full. Publisher: Tree-Ring Society.

[7] David G. Lowe. Distinctive Image Features from Scale-Invariant Keypoints. *International Journal of Computer Vision*, 60(2):91–110, November 2004. ISSN 0920-5691. doi: 10.1023/B:VISI.0000029664.99615.94. URL http://link.springer.com/10.1023/B:VISI.0000029664.99615.94.

[8] Hashim Mir, Peter Xu, and Peter Van Beek. An extensive empirical evaluation of focus measures for digital photography. page 90230I, San Francisco, California, USA, March 2014. doi: 10.1117/12.2042350. URL http://proceedings.spiedigitallibrary.org/proceeding.aspx?doi=10.1117/12.2042350.

[9] Fatemeh Sadat Mohammadi, Hasti Shabani, and Mojtaba Zarei. Fast and robust feature-based stitching algorithm for microscopic images. *Scientific Reports*, 14(1): 13304, June 2024. ISSN 2045-2322. doi: 10.1038/s41598-024-61970-y. URL https://www.nature.com/articles/s41598-024-61970-y. Publisher: Nature Publishing Group.

[10] Jeremy L. Muhlich, Yu-An Chen, Clarence Yapp, Douglas Russell, Sandro Santagata, and Peter K. Sorger. Stitching and registering highly multiplexed whole-slide images of tissues and tumors using ASHLAR. *Bioinformatics (Oxford, England)*, 38(19): 4613–4621, September 2022. ISSN 1367-4811. doi: 10.1093/bioinformatics/btac544.

[11] Aidan O'Dwyer. A Summary of PI and PID Controller Tuning Rules for Processes with Time Delay. Part 1: PI Controller Tuning Rules. *IFAC Proceedings Volumes*, 33(4):159–164, April 2000. ISSN 1474-6670. doi: 10.1016/S1474-6670(17)38237-X. URL https://www.sciencedirect.com/science/article/pii/S147466701738237X.

[12] Sarah Propst and Jochen Mueller. Time Code for multifunctional 3D printhead controls. *Nature Communications*, 16(1):1035, January 2025. ISSN 2041-1723. doi: 10.1038/s41467-025-56140-1. URL https://www.nature.com/articles/s41467-025-56140-1. Publisher: Nature Publishing Group.

[13] Sung-Hyok Ro and Se-Hun Kim. An image stitching algorithm for the mineralogical analysis. *Minerals Engineering*, 169:106968, August 2021. ISSN 0892-6875. doi: 10.1016/j.mineng.2021.106968. URL https://www.sciencedirect.com/science/article/pii/S0892687521001977.

[14] William J Robinson and Robert Evans. A MICROCOMPUTER -BASED TREE -RING MEASURING SYSTEM.

[15] Paul R. Sheppard. Dendroclimatology: extracting climate from trees. *WIREs Climate Change*, 1(3):343–352, 2010. ISSN 1757-7799. doi: 10.1002/wcc.42. URL https://onlinelibrary.wiley.com/doi/abs/10.1002/wcc.42. _eprint: https://onlinelibrary.wiley.com/doi/pdf/10.1002/wcc.42.

[16] A. Park Williams, Joel Michaelsen, Steven W. Leavitt, and Christopher J. Still. Using Tree Rings to Predict the Response of Tree Growth to Climate Change in the Continental United States during the Twenty-First Century. December 2010. doi: 10.1175/2010EI362.1. URL https://journals.ametsoc.org/view/journals/eint/14/19/2010ei362.1.xml. Section: Earth Interactions.